

Polarized-unpolarized ground state of small polycyclic aromatic hydrocarbons

E. San-Fabián and F. Moscardó

Departamento de Química Física, Unidad Asociada del Consejo Superior de Investigaciones Científicas and Instituto Universitario de Materiales, Universidad de Alicante. San Vicente del Raspeig, Alicante 03690, Spain.

(Dated: September 22, 2014)

Do polyacenes, circumacenes, periacenes, nanographenes and graphene nanoribbons show a spin polarized ground state? In this work, we present mono-determinantal (Hartree-Fock and Density Functional Theory types), and multi-determinantal calculations (Møller-Plesset and Coupled Cluster), for several families of unsaturated organic molecules (n-Acenes, n-Periacenes and n-Circumacenes).

All HF calculations and many DFT show a spin-polarized (antiferromagnetic) ground state, in agreement with previous calculations. Nevertheless, the multi-determinantal calculations, carried out with perturbative and variational wavefunctions, show that the more stable state is obtained starting from the unpolarized Hartree-Fock wavefunction.

The trend of the stabilisation of wavefunctions (polarized or unpolarized) with respect to exchange and correlation potentials, and to the number of benzene rings, has been analysed. A study of the spin ($\langle \hat{S}^2 \rangle$) and the spin density on the carbon atoms has also been carried out.

Key words: Spin-polarized states; DFT calculations; MP3; CCSD.

I. INTRODUCTION.

Graphene nanoribbons have been the focus of much research both from experimental and theoretical points of view (See for example ref. [1] and their references), and their magnetic properties have motivated the interest in the study of other small polycyclic aromatic hydrocarbons (PAH). Actually, the ground state of *n*-acenes (*n*-Ac), *n*-periacenes (*n*-PA) and *n*-circumacenes (*n*-CA) molecules has been recently studied by using several methods [2–13], and the principal conclusion of DFT calculations is that they lead to a spin-polarized (antiferromagnetic) ground state for PAH greater than bysanthene[3] and for polyacenes with $n > 7$ [2].

In Fig. 1, the scheme of the 10-Ac, 3-PA and 2-CA molecules is shown, where the growing line is taken along the horizontal axis. The spin-polarisation appears along the molecular growing line, as alternative lines of α and β spins, leading to an antiferromagnetic structure, in agreement with Lieb's theorem [14].

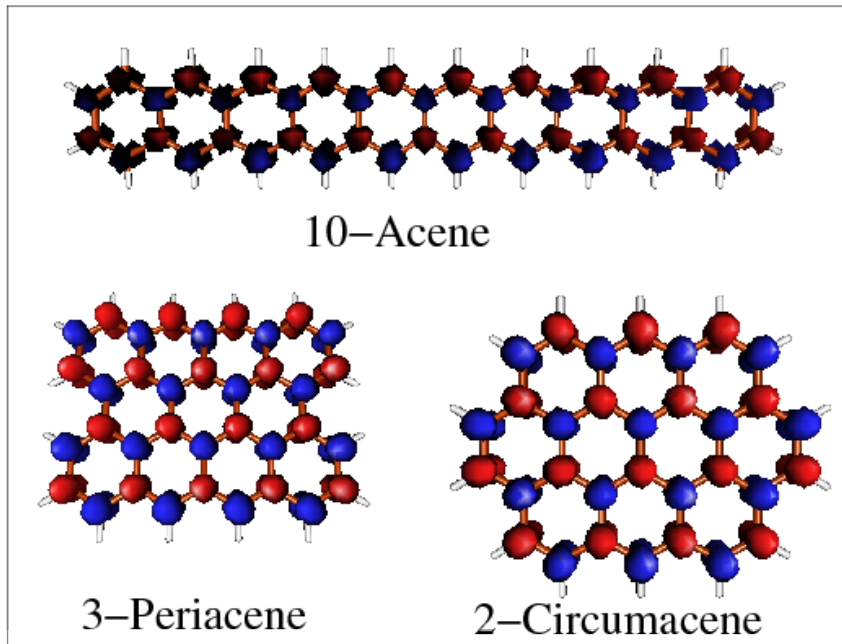


FIG. 1. (colour online) Structure scheme, contour plots of spin densities ($\rho_\alpha - \rho_\beta$) on atoms, for the 10-Ac, 3-PA and 2-CA molecules. Blue and red colors are for the α and β spins, respectively. Results from spin-polarized HF calculations by using the 3-21G basis set[21].

Experimental studies show the existence of magnetism in activated carbon fibers, this fact being interpreted as the presence of *n*-PA nanoribbons exhibiting a spin-polarized structure [15, 16]. The above results from DFT calculations support this interpretation, and it has been argued that DFT methods may become of great utility to investigate this class of nano-materials.

In reference [12], where we reported calculations including part of the correlation energy, we conjectured that the antiferromagnetic states that were produced by the UHF and DFT calculations for the family of *n*-periacene molecules, could be a consequence of the symmetry breaking that occurs in an unrestricted calculation [17–19], and that this description would disappear when the electronic correlation is included.

In a second paper[13] we performed very precise calculations on cyclobutadiene and benzene molecules, prototypes of antiaromatic and aromatic systems, respectively. For both molecules the UHF calculations provided ground electronic states with an antiferromagnetic spin distribution, associated with $M_s = 0$. The subsequent inclusion of the electronic correlation was carried out by two very different procedures. On one side Møller-Plesset perturbative calculations up to four order, with spin projections (SPMP4), were done, and on the other side, we carried out Coupled Cluster calculations including up to quintuple excitations (CCSDTQP).

Both sets of calculations led to similar results for the two molecules, providing states with $\hat{S}^2 = 0$ in which the spin density disappears and with the same energy that the restricted calculations, showing that the antiferromagnetism depicted by the UHF and UDFT calculations is not supported by the results of an accurate theory.

Unfortunately, calculations of the quality of ref.[13] are not accessible for larger molecules, such as those belonging to the family of the *n*-acene and even less for the *n*-periacene and *n*-circumacene families, but the common sense suggests that the conclusions reached in [13], with regard to the nonexistence of the antiferromagnetic solutions, can be extrapolated to these larger systems.

However, there is information in the previous calculations that can be used for a study of more complex systems: In the first stage of correction of the UHF results, the inclusion of electronic correlation produces an reversal of the results, stabilizing the closed shell solution respect to the antiferromagnetic and reducing in an important quantity the values of $\langle \hat{S}^2 \rangle$ and spin densities.

In this paper we show results for a large number of molecules belonging to the families of the n-Ac, n-PA and n-CA, by using unrestricted calculations, without and with forcing the symmetry breaking, together with his perturbative Møller Plesset (MP3), and Coupled Clusters (CCSD) corrections. Likewise, and in order to analyze the importance of the local, non-local, exchange ratio (see ref.[20]), DFT calculations have been made in both with and without broken symmetry forms, considering an extensive variety of exchange functionals, ranging from the non-local HF theory, to the local $X\alpha$ theory.

II. METHOD.

18 molecules belonging to the n-Ac (n=1-10), n-PA (n=1-4) and n-CA(n=1-3, and the pyrene as n=0) families have been studied. The calculations were done using the 3-21G basis set [21], which has proved to be adequate for the present purpose, because, as we can see in ref. [13], the effect to study here it is not basis set dependent,

The GAMESS[22], GAUSSIAN[23] and CFOUR[24] packages, together with the Gabedit[25] and Molden[26] graphical interfaces, have been used.

With respect to the methods of calculation, we have used several exchange functionals: The non-local exchange Hartree-Fock (HF), the meta-GGA functional TPSS[27], which includes $\nabla^2\rho$ and $\nabla\rho$ terms, the GGA functional HCTC/407_{ex}[28], B88[29], and PBE[30], and the local exchange $X\alpha$ [31] functional. The dynamic correlation energy has been included with the Lee-Yang-Parr[32] correlation functional, for the HF and B88 exchange functionals (HF-LYP and BLYP), and by the respective correlation functional in the rest of exchange functional (TPSSTPSS, HCTC/407 and PBE-PBE).

Finally, in order to show the effect of the percentage of the exact exchange in the appearance of antiferromagnetism, we have applied the following hybrid functionals: BhandHLYP (50%HF)[33], PBE1PBE (25%HF)[34] and B3LYP(20%HF)[35]

In a last step, the HF results have been corrected by the correlation energies obtained by using perturbative Møller Plesset (MP3), and Coupled Clusters (CCSD) calculations, using not only the ground state monodeterminantal wavefunction, but their excited ones.

All calculations were carried out at the unrestricted level, with the $M_s = 0$ constraint, and using two different molecular orbital guesses. The calculations made with all the above methods, following an standard route (with auto-generation of the guess for the molecular orbitals) lead always to an unpolarized closed-shell ground state. The antiferromagnetic results have been obtained by following the prescriptions of ref.[12], in which a polarized guess has been used. This guess has been artificially constructed polarising the most external π -molecular orbitals of a closed shell guess, along the growing line of Fig. 1, with the final polarized orbitals resulting from the usual self-consistent procedure.

Having into account that $M_s = 0$ has been imposed for all the calculations shown in this paper, no other polarized states, such as a ferromagnetic, can be expected. Therefore, we are restricted to a diamagnetic closed shell state, and to an antiferromagnetic spin polarized open shell state, corresponding to each of the two stationary states found here.

For all molecules, a fixed geometry, in this case we used the B3LYP optimized geometry found for the unpolarized wavefunction, but the relative results are invariants in respect to the equilibrium geometry considered.

III. CALCULATIONS AND RESULTS

In Tables I and II, the stabilization energies of the spin-polarized solution, with respect to the unpolarized one ($\Delta_{pol-unpol}$), are shown. Where there is no data, it is because there is not a spin-polarized result. The outputs are ordered by following the criterion of the threshold for which the antiferromagnetism appears.

The first row of these tables shows the well-known fact that HF theory predicts the antiferromagnetic wavefunction to be the most stable one, increasing the energy difference between both with the size of the analyzed system. In the second row the results of the HF-LYP calculations, which include the dynamic electron correlation through the LYP functional, are shown. Its effect on HF is to reduce the $\Delta_{pol-unpol}$, but in no case reverses the order of stability.

Rows 3-5 correspond to hybrid functionals, ordered by a decreasing amount of the non-local exchange percentage in the order (BhandHLYP (50%HF), PBE1PBE (25%HF) and B3LYP(20%HF)). The results reveal the fact that the threshold at which the antiferromagnetism appears is linked to the ratio of exact exchange included[12, 20].

The other DFT functionals have been splitted into two groups: Those which consider exclusively the exchange functional, and those which include both, exchange and correlation functionals.

For the first elements of all families the DFT functionals analysed do not produce any polarized wavefunction, but from a threshold in the number of benzene rings, again the spin-polarized solution appears being more stable than the unpolarized ones.

TABLE I. Stabilization energy (in hartree) of the spin-polarized solution versus the unpolarized ($\Delta_{pol-unpol}$). Only when the two solutions are found.

	Benzene	Naphthalene	Anthracene	4-Ac	5-Ac	6-Ac	7-Ac	8-Ac	9-Ac	10-Ac
HF	0.00392	0.01625	0.03649	0.06129	0.08887	0.11823	0.14854	0.17954	0.21096	0.24291
HF-LYP	0.00009	0.00457	0.01660	0.03364	0.05367	0.07552	0.09835	0.12188	0.14583	0.25434
BHandHLYP				0.00046	0.00437	0.01063	0.01797	0.02584	0.03400	0.04239
PBE1PBE						0.00080	0.00353	0.00720	0.01127	0.01552
B3LYP						0.00001	0.00128	0.00382	0.00694	0.01030
TPSS						0.00015	0.00186	0.00468	0.00802	0.01156
B88							0.00034	0.00206	0.00458	0.00746
HCTH/407 _{ex}							0.00030	0.00200	0.00455	0.00747
PBE							0.00017	0.00166	0.00402	0.00680
X α								0.00049	0.00224	0.00467
TPSSTPSS							0.00011	0.00151	0.00388	0.00671
BLYP								0.00008	0.00124	0.00325
HCTH/407								0.00063	0.00243	0.00482
PBEPBE								0.00018	0.00156	0.00374
MP3	-0.02268	-0.04686	-0.06552	-0.07933	-0.09049	-0.10048	-0.10971	-0.11854	-0.12711	-0.13547
CCSD	-0.00279	-0.00772	-0.01271	-0.01565	-0.01612	-0.01486	-0.01263	-0.00986	-0.00681	-0.00349

TABLE II. Stabilization energy (in hartree) of the spin-polarized solution versus the unpolarized ($\Delta_{pol-unpol}$). Only when the two solutions are found.

	Perylene	2-PA	3-PA	4-PA	Pyrene	1-CA	2-CA	3-CA
HF	0.05429	0.11050	0.17340	0.23656	0.03751	0.05836	0.09290	0.29693
HF-LYP	0.02568	0.06706	0.11615	0.16570	0.01572	0.02519	0.04638	0.24675
BHandHLYP		0.00659	0.02519	0.04439				0.06049
PBE1PBE		0.00002	0.00803	0.01967				0.02830
B3LYP			0.00476	0.01466				0.02200
TPSS			0.00352	0.01117				0.01671
B88			0.00149	0.00783				0.01273
HCTH/407 _{ex}			0.00142	0.00783				0.01280
PBE			0.00118	0.00728				0.01210
X α			0.00028	0.00528				0.00981
TPSSTPSS			0.00105	0.00725				0.01224
BLYP			0.00003	0.00407				0.00839
HCTH/407			0.00042	0.00567				0.01033
PBEPBE			0.00008	0.00449				0.00892
MP3	-0.09049	-0.11029	-0.12381	-0.07427	-0.07506	-0.11237	-0.14452	-0.15685
CCSD	-0.01800	-0.01667	-0.00487	0.00547	-0.01439	-0.02160	-0.02788	0.01558

The relative stability of the spin-polarized and unpolarized wavefunctions is reversed, being in agreement with the results of reference [13]. In these calculations there are two exceptions for 4-PA and 3-CA systems discussed next.

In Table III we reproduce the values of $\langle \hat{S}^2 \rangle$ and spin density on the most polarized carbon atom ($\rho_s(C)$), obtained with the HF and the CCSD spin-polarized calculations. The reduction in the values of $\langle \hat{S}^2 \rangle$ and $\rho_s(C)$ is noticeable when going from the HF level to the CCSD one.

In Table III it is also shown the norm of the CCSD wavefunctions (Norm(A)). Since the coefficient of the reference determinant in the CCSD wavefunction is 1.0, the norm is directly related to the modification of the reference wavefunction by the CCSD correction. The last column of this Table shows the percentage in which the $\langle \hat{S}^2 \rangle$ is corrected by the CCSD contributions. The norm values show that the CCSD weight into the wavefunction grows with the size of the molecule. But the last column of Table III shows also that the correlation correction provided by the CCSD contribution is less effective when the size of the molecule grows. This result may explain the behaviour pointed above on the 4-PA and 3-CA results.

The trends shown by the $\Delta_{pol-unpol}$, $\langle \hat{S}^2 \rangle$ and $\rho_s(C)$, collected in Tables I-III, are the same as those exhibited by the smaller systems of ref. [13], and if it is supposed that the trend is maintained as the correlation included into the wavefunction grows, as is also the case in ref. [13], then it can be assumed that the antiferromagnetism disappears for the exact wavefunction, and that it is an artifact associated with the broken symmetry of the unrestricted results (HF, DFT, MP3 and CCSD).

TABLE III. The $\langle \hat{S}^2 \rangle$ and the spin-density on the most polarized carbon atom ($\rho_s(C)$) values of HF and CCSD calculations, and the norm (Norm(A)), and percentage of the $\langle \hat{S}^2 \rangle$ reduction of CCSD calculations, for the spin-polarized wavefunctions. All in a.u.

	HF		CCSD			
	$\langle \hat{S}^2 \rangle$	$\rho_s(C)$	$\langle \hat{S}^2 \rangle$	$\rho_s(C)$	Norm(A)	% $\langle \hat{S}^2 \rangle$
Benzene	0.4926	0.7034	0.0099	0.0609	1.1848	97.99
Naphthalene	1.1573	0.8578	0.0571	0.0444	1.3064	95.07
Anthracene	1.8441	0.9883	0.1847	0.2202	1.4019	89.75
4-Acene	2.5133	1.0121	0.4038	0.3368	1.4777	83.94
5-Acene	3.1662	1.0334	0.6657	0.4489	1.5471	78.97
6-Acene	3.8165	1.0411	0.9252	0.4897	1.6154	75.76
7-Acene	4.4648	1.0451	1.1699	0.5237	1.6882	73.80
8-Acene	5.1130	1.0489		0.5311	1.7464	
9-Acene	5.7604	1.0501			1.8087	
10-Acene	6.4076	1.0514			1.8688	
Perylene	2.6381	1.0376	0.3230	0.2107	1.5259	87.76
2-Periacene	3.9051	1.1259	0.8797	0.4502	1.6432	77.47
3-Periacene	5.1097	1.1298		0.5262	1.7684	
4-Periacene	6.3013	1.1323			1.8907	
Pyrene	2.0415	0.9936	0.1873	0.1546	1.4411	90.83
1-Circumacene	3.0792	1.0427	0.3064	0.1694	1.6022	90.05
2-Circumacene	4.2467	1.0969		0.3088	1.7039	
3-Circumacene	7.4917	1.1390				

IV. CONCLUSIONS.

The three studied families show an antiferromagnetic ground state at the HF level. The incorporation of the dynamic correlation through the LYP method, does not change this behavior, although it reduces the energy difference between the spin-polarized and unpolarized solutions.

Calculations performed with the functionals belonging to several DFT models, show that the threshold at which the antiferromagnetic solution appears, depends on the percentage of local exchange present in the functional, and, in accordance with previous findings[20], it is shifted to larger values of n as the percentage of HF exchange diminishes, and the polarisation effect decreases.

For the set of DFT functionals having not a HF exchange component, i.e. the non-hybrid ones, a similar, although quite more mild, behaviour is found. The highest value of n for the threshold is obtained for the X_α functional, being followed by the gradient functionals, with the functional having an explicit dependence in the second derivative of the density being the last. This result is interesting since it suggests that a Taylor correction around the local approximation for the exchange mimics, although moderately, the non-locality component of the exact functional.

The effect of including the dynamic correlation by adding it to the above DFT functionals, acts in the same way as that observed for the HF results.

The inclusion of part of the correlation energy on the HF solutions, at the MP3 and CCSD levels, reverses the order of the stability of both solutions and now, the ground state is the unpolarized wavefunction. This change in the relative stability is accompanied by a decrease in the $\langle \hat{S}^2 \rangle$ and $\rho_s(C)$ values for the antiferromagnetic results. The exceptions found in the CCSD calculations, for the 4-PA and 3-CA, together with the trend of the $\langle \hat{S}^2 \rangle$ and $\rho_s(C)$ values shown in Table III suggest the need to incorporate higher excitations, to remove the larger spin contamination that appears as n grows.

The comparison between the three families studied supports the conclusion that PAHS, the molecular size and geometry have a strong influence on their theoretical results.

Finally, from these calculations appear to confirm and expand the preliminary results of ref. [13], in the sense that the antiferromagnetism of the three families of hydrocarbons discussed in this paper tends to disappear when considering wavefunctions beyond monodeterminantal solution.

ACKNOWLEDGMENTS

Financial support by the Spanish MCYT (grants FIS2008-06743 and FIS2009-10325) and the Universidad de Alicante is gratefully acknowledged

-
- [1] Yan, X.; Cui, X.; Li, B.; Li, L.-s. *Nano Letters* 2010, 10, 1869.
- [2] Jiang, D.-e.; Dai, S. *J. Phys. Chem. A* 2008, 112, 332.
- [3] Jiang, D.-e.; Sumpter, B. G.; Dai, S. *J. Chem. Phys.* 2007, 127, 124703.
- [4] Jiang, D.-e.; Dai, S. *Chem. Phys. Letters* 2008, 466, 72.
- [5] Hod, O.; Barone, V.; Scuseria, G. E. *Phys. Rev. B* 2008, 77, 035411.
- [6] Zheng, H.; Duley, W. *Phys. Rev. B* 2008, 78, 155118.
- [7] Qu, Z.; Zhang, D.; Liu, C.; Jiang, Y. *J. Phys. Chem. A* 2009, 113, 7909.
- [8] Bendikov, M.; Duong, H. M.; Starkey, K.; Houk, K. N.; Carter, E. A.; Wudl, F. *J. Am. Chem. Soc.* 2004, 126, 7416.
- [9] Aihara, J.I. *Phys. Chem. Chem. Phys.* 1999, 1, 3193.
- [10] Hajgató, B.; Deleuze, M. S.; Tozer, D. J.; Proft, F. D. *J. Chem. Phys.* 2008, 129, 084308.
- [11] Hajgató, B.; Huzak, M.; Deleuze, M. S. *J. Phys. Chem. A* 2011, 115, 9282.
- [12] Moscardó, F.; San-Fabián, E. *Chem. Phys. Letters* 2009, 480, 26.
- [13] San-Fabián, E.; Moscardó, F. *Eur. Phys. J. D* 2011, 64, 239.
- [14] Lieb, E. H. *Phys. Rev. Lett.* 1989, 62, 1201.
- [15] Shibayama, Y.; Sato, H.; Enoki, T.; Endo, M. *Phys. Rev. Lett.* 2000, 84, 1744.
- [16] Enoki, T.; Kobayashi, Y. *J. Mater. Chem.* 2005, 15, 3999.
- [17] Bagus, P. S.; Bennett, B. I. *Int. J. Quantum Chem.* 1975, 9, 143.
- [18] Noodleman, L.; Davidson, E. R. *Chem. Phys.* 1986, 109, 131.
- [19] Noodleman, L. *J. Chem. Phys.* 1981, 74, 5737.
- [20] Rudberg, E.; Salek, P.; Luo, Y. *Nano Letters* 2007, 7, 2211.
- [21] Binkley, J. S.; Pople, J. A.; Hehre, W. J. *J. Am. Chem. Soc.* 1980, 102, 939.
- [22] Schmidt, M.W. et al., *J. Comput. Chem.* 1993, 14, 1347.
- [23] Frisch, M. J. et al., *Gaussian 09 Revision A.1.* Gaussian Inc. Wallingford CT 2009.
- [24] Coupled-cluster techniques for computational chemistry, a quantum-chemical program package by Stanton J.F.; Gauss J.; Harding M.E.; Szalay P.G. with contributions from Auer A.A.; Bartlett R.J.; Benedikt U.; Berger C.; Bernholdt D.E.; Bomble Y.J.; Christiansen O.; Heckert M.; Heun O.; Huber C.; Jagau T.-C.; Jonsson D.; JusÅl'lius J.; Klein K.; Lauderdale W.J.; Matthews D.A.; Metzroth T.; O'Neill D.P.; Price D.R.; Prochnow E.; K. Ruud K.; Schifmann F.; Stopkowicz S.; Tajti A.; Vázquez J.; Wang F.; Watts J.D. and the integral packages molecule (AlmlÅuf J. and Taylor P.R.), props (Taylor P.R.), abacus (Helgaker T.; Jensen H.J. AA.; JÅyrgensen P.; and Olsen J.), and ecp routines by Mitin A. V. and van WÅijllen C.. for the current version, see <http://www.cfour.de>.
- [25] Gabedit is a free graphical user interface for computational chemistry packages of Allouche, A.R.. See also <http://gabedit.sourceforge.net/>.
- [26] Schaftenaar, G.; Noordik, J. *J. Comput.-Aided Mol. Design* 2000, 14, 123.
- [27] Tao, J.; Perdew, J. P.; Staroverov, V. N.; Scuseria, G. E. *Phys. Rev. Lett.* 2003, 91, 146401.
- [28] Boese, A. D.; Handy, N. C. *J. Chem. Phys.* 2001, 114, 5497.
- [29] Becke, A. D. *Phys. Rev. A* 1988, 38, 3098.
- [30] J. P. Perdew, K. B.; Ernzerhof, M. *Phys. Rev. Lett.* 1996, 77, 3865.
- [31] Slater, J. *The Self-Consistent Field for Molecular and Solids, Quantum Theory of Molecular and Solids*; McGraw-Hill: New York, 1974.
- [32] Lee, C.; Yang, W.; Parr, R. G. *Phys. Rev. B* 1988, 37, 785.
- [33] Becke, A. D. *J. Chem. Phys.* 1993, 98, 1372.
- [34] Adamo, C.; Barone, V. *J. Chem. Phys.* 1999, 110, 6158.
- [35] Becke, A. D. *J. Chem. Phys.* 1993, 98, 5648.